Does the S2 Rod of Myosin II Uncoil upon Two-Headed Binding to Actin? A Leucine-Zippered HMM Study†

Tania Chakrabarty,‡,⊥ Chris Yengo,§ Corry Baldacchino,§ Li-Qiong Chen,§ H. Lee Sweeney,*,§ and Paul R. Selvin*,‡,||

Center for Biophysics and Computational Biology and Physics Department, University of Illinois, Urbana, Illinois 61801, and Department of Physiology, University of Pennsylvania School of Medicine, 3700 Hamilton Walk, Philadelphia, Pennsylvania 19104-6085

Received July 2, 2003; Revised Manuscript Received September 11, 2003

ABSTRACT: Myosin II, like many molecular motors, is a two-headed dimer held together by a coiled-coil rod. The stability of the (S2) rod has implications for head−head interactions, force generation, and possibly regulation. Whether S2 uncoils has been controversial. To test the stability of S2, we constructed a series of "zippered" dimeric smooth muscle myosin II compounds, containing a high-melting temperature 32-amino acid GCN4 leucine zipper in the S2 rod beginning 0, 1, 2, or 15 heptads from the head−rod junction. We then assessed the ability of these and wild-type myosin to bind strongly via two heads to an actin filament by measuring the fluorescence quenching of pyrene-labeled actin induced by myosin binding. Such two-headed binding is expected to exert a large strain that tendd to uncoil S2, and hence provide a robust test of S2 stability. We find that wild-type and zippered heavy meromyosin (HMM) are able to bind by both heads to actin under both nucleotide-free and saturating ADP conditions. In addition, we compared the actin affinity and rates for the 0- and 15-zippered HMMs in the phosphorylated "on" state and found them to be very similar. These results strongly suggest that S2 uncoiling is not necessary for two-headed binding of myosin to actin, presumably due to a compliant point in the myosin head(s). We conclude that S2 likely remains intact during the catalytic cycle.

Myosin II, like many molecular motors, is a two-headed dimer held together by a coiled-coil rod. Each myosin heavy chain of the dimer can be divided into two subfragments on the basis of proteolytic digestion studies of myosin. Subfragment 1 (S1) consists of the N-terminal end of myosin, which forms a globular domain with the actin- and ATP-binding sites. Subfragment 2 (S2)[1] consists of the C-terminal end, which forms the coiled-coil rod. In addition, two light chains, the essential light chain and regulatory light chain, bind on the heavy chain near the head−rod junctions (see Figure 1). The rod has a repeating pattern of seven amino acids, or heptads, with hydrophobic residues in the **a** and **d** positions so that the coiled coil is stabilized by interactions along this hydrophobic interface.

The stability of the S2 rod, and in particular, whether S2 uncoils, has implications for head−head interactions, force generation, and regulation of myosin's motor activity. For example, Trybus et al. (*1*) recently concluded that uncoiling of S2 was necessary for optimal mechanical performance of smooth muscle myosin. Regulation of smooth muscle myosin is also dependent on S2: phosphorylation and dephosphorylation of the regulatory light chain of myosin fully turn myosin's ATPase activity on and off, respectively, only if both myosin heads and a rod of at least 15 heptads are present (*2*).

The stability of the S2 rod toward uncoiling has been controversial. Several studies, based on dimerization stability and negatively stained electron microscopy, have been interpreted to indicate that smooth muscle S2 likely uncoils (see ref *1* and references therein). However, one cross-linking study suggested that smooth muscle S2 likely remains intact, at least part of the time (*3*), although a more recent cross-linking study by the same group has been interpreted to indicate that the first heptad of S2 may uncoil (*4*). Using fluorescence resonance energy transfer, we recently measured the distance between the regulatory light chains near the head−rod junctions within the skeletal muscle heavy meromyosin (HMM) dimer when bound via two heads to an actin filament (*5*). Double-headed binding of myosin to a single actin filament creates a large strain within the myosin dimer, which may cause S2 to uncoil and separate the head−rod junctions. Even under this large strain, we found that the distances between the RLCs remained short (<50 Å), implying that S2 remained largely coiled, at least beyond the first heptad. This in turn implies that S2 is quite stable and unlikely to uncoil under physiologically relevant strains.

† Supported by NIH Grants AR44420 (P.R.S.) and AR35661 (H.L.S.).

* To whom correspondence should be addressed. E-mail: selvin@uiuc.edu or lsweeney@mail.med.upenn.edu.

‡ Center for Biophysics and Computational Biology, University of Illinois.

§ University of Pennsylvania School of Medicine.

|| Physics Department, University of Illinois.

⊥ Current address: Department of Pharmacology, University of Michigan, Ann Arbor, MI 48109.

[1] Abbreviations: HMM, heavy meromyosin; *n*-zipHMM, smooth muscle heavy meromyosin with a GCN4 leucine zipper *n* heptads from the head−rod junction; skS1, subfragment 1 of skeletal myosin; S2, subfragment 2; RLC, regulatory light chain; skHMM, wild-type skeletal HMM.

10.1021/bi035144f CCC: $25.00
Published on Web 10/17/2003

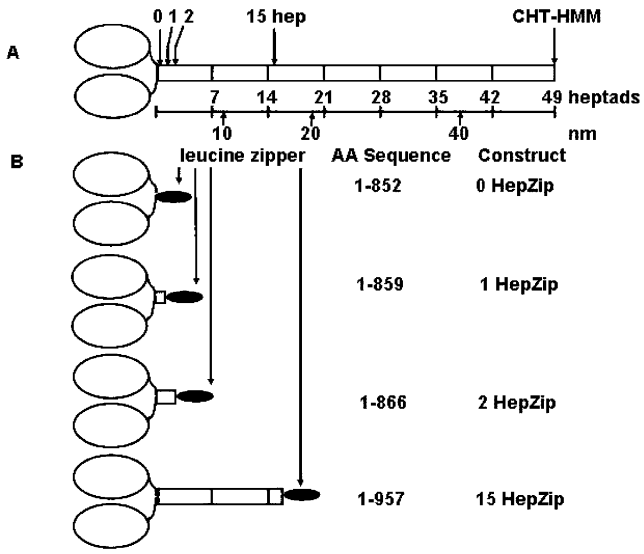

FIGURE 1: (A) Diagram of double-headed heavy meromyosin prepared by chymotryptic digestion (CHT-HMM) (modified from ref *2*). The globular head domain consists of amino acids 1−849 (subfragment 1 or S1) and is followed by the rod sequence, which consists of 49 heptads (subfragment 2 or S2). One heptad consists of seven amino acids (**abcdefg**), where there are hydrophobic residues at the **a** and **d** positions (*25*). The length of the rod is shown based on a rise per residue of 0.15 nm. The head domain is not drawn to scale. (B) Illustration of the C-terminal leucine zipper constructs used in this study. The C-terminal leucine zipper constructs are named for the number of heptads of native rod sequence before the leucine zipper sequence; e.g., a 2-heptad/zipper has two heptads of rod sequence followed by the 31-amino acid leucine zipper sequence. The leucine zipper is represented by a black oval.

To further test whether S2 uncoiling is necessary for two-headed binding to actin, and to extend our previous results on skeletal muscle myosin to smooth muscle myosin, here we have constructed a series of dimeric smooth HMMs, containing a 32-amino acid GCN4 leucine zipper at positions 0, 1, 2, and 15 heptads from the head−rod junction. We have studied their ability to bind via two heads to actin filaments under both nucleotide-free (rigor) and ADP conditions. The S2 rods of these constructs are highly stable. If S2 uncoiling is not necessary for two-headed binding, then these zippered HMMs should be able to bind via two heads, and with affinities similar to that of wild-type HMM. However, if S2 uncoiling is required, then single-headed binding is expected for those myosins zippered up to the rod residue where such a putative uncoiling is required. Fluorescence quenching of pyrene-labeled actin by myosin heads, which provides a spectroscopic signature for one- versus two-headed binding, was used. We find unphosphorylated wild-type heavy meromyosin (HMM) and HMMs zippered 15, 2, 1, and 0 heptads away from the head−rod junction are able to bind by both heads in rigor (no nucleotide) and in the presence of a saturating amount of ADP. The 0- and 15-heptad zippered HMMs were tested when phosphorylated, and these are also able to bind actin via both heads. A stopped-flow quenching experiment shows that the binding constants of the phosphorylated 0- and 15-heptad zippered HMM are experimentally indistinguishable. These results strongly imply that uncoiling of S2 is not necessary for two-headed binding and that S2 likely remains coiled during myosin II's catalytic cycle.

MATERIALS AND METHODS

Myosin Expression. Smooth muscle myosin constructs were expressed in Sf9 cells (baculovirus expression system) as previously described (*2*). Zippered HMMs were made by introducing a 31-amino acid GCN4 leucine zipper (*6*) 0, 1, 2, and 15 heptads after proline 849 located at the head−rod junction (Figure 1). The sequence of the GCN4 leucine zipper, with position **d** of the heptad repeat in bold, is MKQ**L**EDKVEE**L**LSKNYH**L**ENEVAR**L**KKLVGE. To ensure that incorporation of the GCN4 leucine zipper is not disrupting the phase of the S2 rod heptads, the positions of the hydrophobic and ionic charges are maintained at the **a** and **d** and **e** and **g** positions, respectively. The 0-, 1-, 2-, and 15-heptad zipper (hepzip) constructs were truncated after Gln852, Glu859, Glu866, and Gln957, respectively. A FLAG epitope was added at the C-terminus for purification by affinity chromatography using an anti-FLAG column. For steady-state measurements, unphosphorylated myosin was used. For transient measurements, both phosphorylated and unphosphorylated 0- and 15-heptad zippered HMM were used. Phosphorylation of the regulatory light chain was achieved via published procedures using myosin light chain kinase kindly supplied by J. T. Stull (*7*). Native gel electrophoresis to determine the extent of dimerization was carried out according to published methods (*8*). Skeletal HMM, prepared by chymotryptic treatment of myosin, and skeletal S1 were gifts from R. Cooke (University of California, San Francisco, CA).

Actin Labeling. Actin was purified from rabbit skeletal muscle using an acetone powder method and gel filtered (*9*). For labeling, actin was reacted with pyrene iodoacetamide (Molecular Probes) and purified using published protocols (*10*). The extent of labeling was calculated from the absorption spectra. The pyrene-labeled actin (pyrene−actin) was stabilized by addition of phalloidin (1:1 molar ratio) before being used. For experiments performed in rigor (no nucleotide), the phalloidin-stabilized pyrene−actin was treated with apyrase (0.005−0.01 unit, grade VII, Sigma) to remove ATP or ADP. For experiments performed in the presence of ADP, the phalloidin-stabilized pyrene−actin was treated with 20 μM hexokinase and 2 mM glucose to remove ATP.

Steady-State Fluorescence Quenching Measurements. Pyrene-labeled actin was excited at 365 nm, and the fluorescence emission was monitored at 405 nm as a function of added myosin (Jovin Yvon, steady-state Fluoromax 2 fluorimeter). The actin concentration was 0.1−1 μM (typically 0.35−1 μM) in a buffer containing 100 mM KCl, 20 mM MOPS, 5 mM $MgCl_2$, 0.1 mM DTT (pH 7), and 0.1−2 mM ADP, when present. Just prior to titrations, the myosin was centrifuged in an airfuge at 80 000 rpm for 30 min and the supernatant was used after determining the myosin concentration via absorption. The myosin concentration was varied from zero to saturating levels, where pyrene fluorescence quenching reached a steady value. With saturating levels of myosin, the extent of fluorescence quenching of pyrene was typically 75% in rigor and 65% in the presence of ADP. The dilution of pyrene-labeled actin due to titration of myosin heads was typically 8−10%, for which the data analysis was corrected. Actin and myosin concentrations were determined by absorption spectra of stock solutions.

In addition, to further check the actin concentration, a control experiment was carried out by titrating in skHMM and skeletal S1 to confirm two- and one-headed binding, respectively.

Fluorescence quenching of pyrene−actin due to titration with myosin was fit following a method similar to that of Conibear and Geeves (*11*). Specifically, the fluorescence as a function of total myosin concentration, $F([m])$, was analyzed via a nonweighted nonlinear least-squares fitting (Kaleidagraph, Synergy Software):

$$F([m]) = \left(\frac{F_o - F_{max}}{[A]}\right) \times \frac{\beta}{2}\left[\sqrt{\left([m] - \frac{[A]}{\beta} + \frac{1}{K}\right)^2 + \frac{4[A]K}{\beta}} + [m] - \frac{[A]}{\beta} + \frac{1}{K}\right] + F_{max} \quad (1)$$

where F_o is the normalized pyrene fluorescence at zero myosin concentration (theoretically equal to 1, but allowed to float in the curve fit), F_{max} is the pyrene fluorescence at a saturating myosin concentration, [A] is the total actin concentration, K is the binding constant of myosin for actin, and β, the primary variable of interest here, is the stoichiometry of binding, i.e., the number of actin monomers bound per myosin at a saturating myosin concentration. ($\beta = 2$ for double-headed binding and 1 for single-headed binding of myosin to actin; β is closely related though not identical to α in ref *11*.) All parameters except for [A], i.e., F_o, F_{max}, β, [m], and K, were allowed to float in the fitting procedure, although fixing F_o to 1, and F_{max} to the final fluorescence determined by visual inspection, yielded very similar results for β. Initial guesses were provided for all other parameters. The initial guess for β was taken to be 1.5 so as not to bias the expected outcome of 1 or 2; values for K were taken from ref *11*.

Transient Fluorescence Quenching Measurements. All transient kinetic experiments were performed with an Applied Photophysics (Surrey, U.K.) stopped-flow model SX.18MV instrument with a dead time of 1.2 ms. (The dead time was determined under the same conditions used in our experiments.) The instrument was equipped with a 150 W xenon arc lamp as a light source, and a bandwidth of 2 nm was used for all experiments. Pyrene fluorescence was excited at 365 nm, and the emitted fluorescence was measured using a 400 nm long pass filter (Oriel Corp., Stratford, CT). Nonlinear least-squares fitting of the data was done with software provided by the instrument or with Kaleidagraph (Synergy Software, Reading, PA). Uncertainties reported are standard errors of the fit unless stated otherwise. All transient kinetic experiments were performed in 20/20 buffer [20 mM MOPS (pH 7.0), 20 mM KCl, 5 mM $MgCl_2$, 1 mM EGTA, and 1 mM DTT] at 25 °C. The rate of myosin binding to actin filaments was determined by mixing myosin with a 10-fold excess of pyrene−actin over the myosin head concentration in the presence of ADP and measuring the rate of pyrene fluorescence quenching. The actin concentration ranged from 1 to 50 μM.

Kinetic Modeling. Kinetic Scheme 1 (*14*) was used to model the interaction between myosin and pyrene−actin filaments in the presence of MgADP, where A represents actin, M represents myosin, and A* indicates that the pyrene−actin fluorescence is unquenched.

Scheme 1

$$A^* + M.ADP \overset{K_1}{\leftrightarrow} A^*.(M.ADP) \overset{k_{+2}}{\underset{k_{-2}}{\leftrightarrow}} A.M.ADP \overset{K_3}{\leftrightarrow} A.M + ADP$$

The initial collision complex between myosin and actin is thought to be a rapid equilibrium (K_1) process that does not quench pyrene−actin fluorescence, and is followed by an isomerization step (K_2) that results in a strongly bound complex in which the pyrene fluorescence is quenched. The final step is the dissociation of MgADP (K_3), resulting in formation of the nucleotide-free actomyosin complex. However, since our stopped-flow experiments included saturating MgADP concentrations, this last step can be ignored.

The rates of binding to actin were plotted as a function of actin concentration and fit to a rectangular hyperbola whereby $k_{obs} = \text{amplitude}[\text{actin}]/(K_{0.5} + [\text{actin}])$. The linear phase of the curve at low actin concentrations was modeled to be the association rate constant (K_1k_{+2}); the amplitude was equal to the maximum rate (k_{+2}), and $K_{0.5}$ was equal to the actin concentration at which there is half-maximal saturation ($1/K_1$). The rate of dissociation from actin was determined by monitoring the pyrene−actin fluorescence recovery in the presence of excess unlabeled actin. Dissociation of the actin−myosin complex was modeled to be limited by k_{-2}, because k_{-1} is known to be very fast (1000 s^{-1}) (*15*). Therefore, the affinity for actin (K_d) can be determined with the equation $K_d = k_{-2}/K_1k_{+2}$. The free energy of binding (ΔG) then equals $k_BT(\ln K_d)$.

RESULTS

Dimerization State of Zippered Myosins. The dimerization state of the smooth muscle myosin ZipHMM constructs was determined by native gel electrophoresis. All of the smooth muscle myosin ZipHMM constructs were dimerized as demonstrated by a slower rate of migration compared to monomeric smooth muscle myosin S1 (Figure 2). In addition, we found the 15-heptad zippered HMM was fully regulated (data not shown), which requires dimerization. This is in agreement with previous measurements on this construct (*16*).

Steady-State Fluorescence in Rigor (No Nucleotide). Figure 3 shows the quenching of pyrene−actin fluorescence as a function of increasing myosin heads for the 0-, 1-, 2-, and 15-heptad zippered smooth muscle HMMs, and for skeletal wild-type HMM and S1, all under rigor conditions. The data were fit according to eq 1. Data for multiple measurements are summarized in Table 1. Under the conditions that were used, the binding of myosin heads for actin is very strong [K_{eq} for acto-skS1 of $\approx 10^7$, K_{eq} for acto-skHMM of $\approx 10^{10}$ (*17*), and K_{eq} for smooth S1 and HMM in rigor of $\gg 2.5 \times 10^7$ (*18*)], and essentially all heads capable of binding to actin are bound. Hence, two-headed binding of HMM leads to saturation of 0.5 HMM per actin monomer, and one-headed binding of S1 leads to saturation at one S1 per actin monomer. The wild-type skHMM and skS1 serve as controls and display the expected two-headed and one-headed binding, respectively. The actin concentrations were chosen such that the two HMM heads bind to adjacent actin monomers on the same actin filament [[actin] $\ll$ 100 μM (*11*)]. The titrations of the zippered HMMs nearly overlap

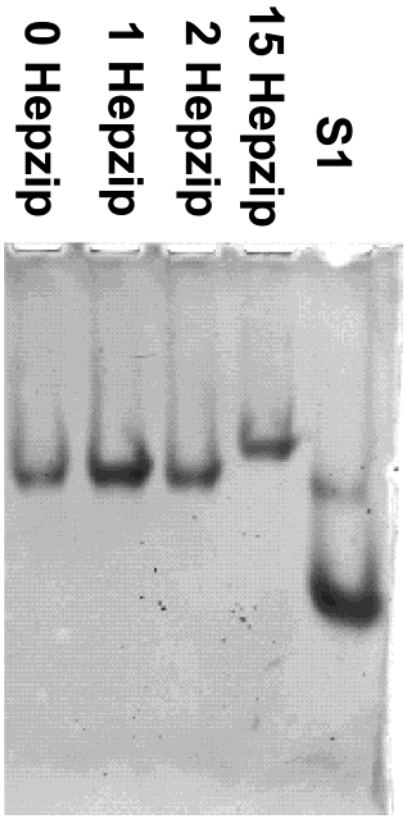

FIGURE 2: Native gel electrophoresis of leucine-zippered smooth muscle HMM (HepZip) constructs. All of the zippered HMM constructs (lanes 1−4) migrate considerably slower than monomeric smooth muscle myosin S1 (lane 5), indicating the HMMs are dimerized.

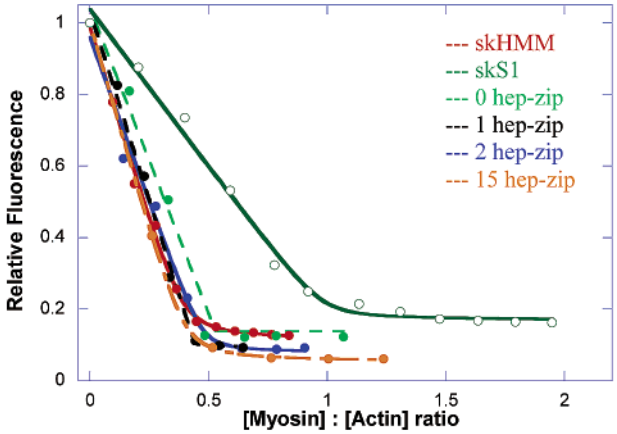

FIGURE 3: Steady-state pyrene−actin fluorescence quenching in rigor upon titration with myosin. The skeletal HMM and S1 controls show the expected two- and one-headed binding, respectively. All zippered HMMs show two-headed binding. The actin concentration was ~1 μM. Lines represent curve fits to eq 1.

that of the wild-type skHMM and are readily distinguishable from the one-headed skS1 control. This clearly shows that the zippered HMMs can bind via two heads to actin filaments under rigor conditions.

Steady-State Fluorescence with ADP. Figure 4 shows a titration of zipper smooth HMM in the presence of a saturating concentration (200 μM) of ADP. It is clear that the zippered HMMs are able to bind by both heads to actin. Titrations with ADP in the range of 50−300 μM (and 2 mM rarely) were also performed and led to essentially identical

Table 1: Steady-State Fluorescence Quenching of Pyrene-Labeled Actin by Myosin[a]

sample	stoichiometry in rigor	stoichiometry in the presence of ADP[b]
skHMM	1.96 ± 0.234 (n = 11)	*c*
skS1	0.86 ± 0.175 (n = 7)	*c*
0hep	2.17 ± 0.36 (n = 13)	2.21 ± 0.28 (n = 6)
1hep	2.005 ± 0.35 (n = 4)	2.09 ± 0.153 (n = 3)
2hep	2.46 ± 0.22 (n = 3)	2.42 (n = 1)
15hep	2.33 ± 0.35 (n = 4)	1.88 ± 0.2 (n = 4)

[a] Values represent the ratios of actin binding sites to myosin ([S1] or [HMM]) at saturation (β, eq 1), derived from curve fits via eq 1. The uncertainties are standard deviations. [b] The ADP concentration was at saturating levels, either 100 or 200 μM. Experiments at 350 μM and 2 mM ADP gave the same results. [c] For skeletal HMM and S1 (skHMM and skS1, respectively) in the presence of a saturating concentration of ADP, there was a weakening of the binding to actin. Under these conditions, an equilibrium between one- and two-headed binding for skHMM was observed.

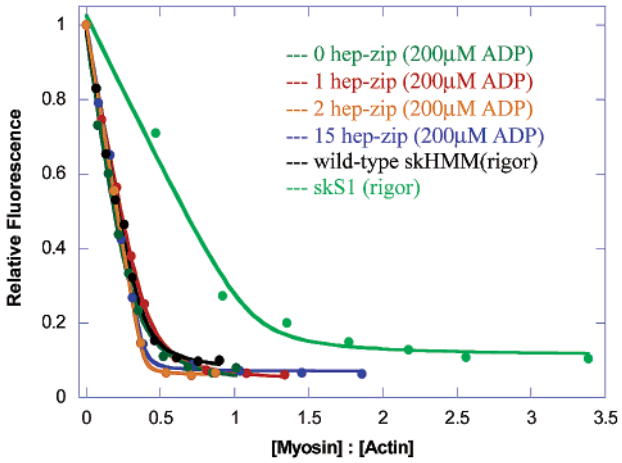

FIGURE 4: Steady-state pyrene−actin fluorescence quenching by myosin in 200 μM ADP. The titration with myosin shows two-headed binding of zippered HMM and wild-type skHMM and one-headed binding of the skS1 control. The concentration of actin was 0.5 μM. Lines represent curve fits to eq 1.

graphs (data not shown). Data for multiple measurements are summarized in Table 1.

Transient Measurements. The plots of the rates of actin binding as a function of actin concentration for the 0- and 15-heptad zipper HMM constructs in both the phosphorylated and dephosphorylated states are shown in Figure 5, and the rate and equilibrium constants are summarized in Table 2. In all cases, the pyrene−actin fluorescence transients were best fit to a single exponential. The rate of dissociation from pyrene−actin was quite similar in all the HMM constructs (~0.006−0.008 s^{-1}) (Table 2).

The rates of binding to actin of the 0- and 15-heptad zipper HMM constructs in the phosphorylated state exhibited a similar dependence on actin concentration. The actin association rates, the rate at which half-maximal saturation was reached, and the affinity for actin were quite similar (Table 2). The maximal rate of actin binding was slightly higher for the 0-heptad zipper HMM than for the 15-heptad zipper HMM (k_{+2} = 19.0 ± 0.4 and 13.9 ± 1.0 s^{-1}, respectively). In addition, the maximum rate of binding of the 15-heptad zipper HMM was slightly higher than that reported for the proteolytically prepared smooth muscle myosin HMM (k_{+2} = 9.0 ± 0.9 s^{-1}) (*16*).

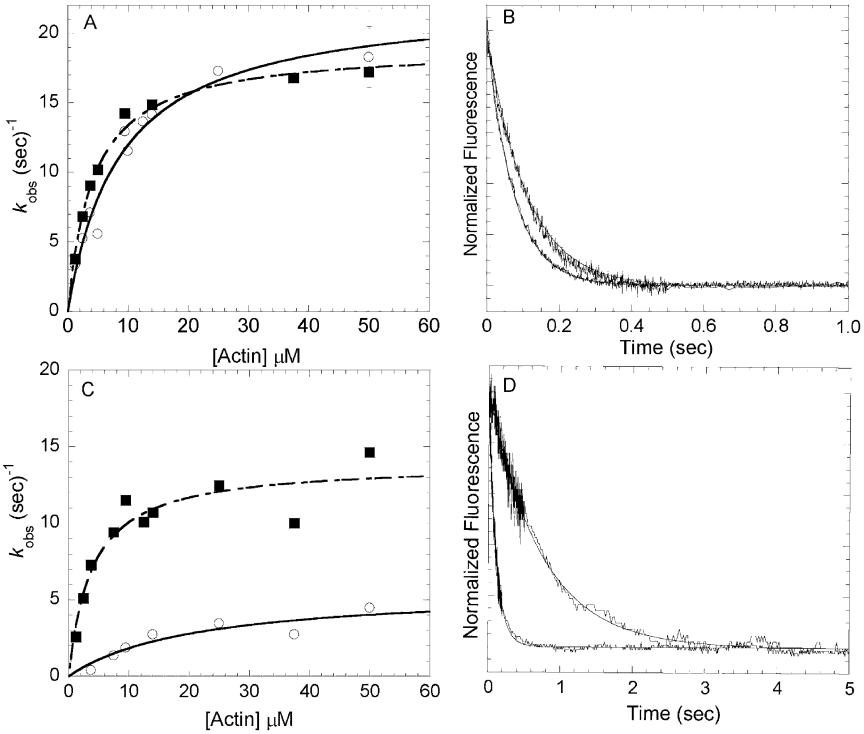

FIGURE 5: Kinetics of 0- and 15-heptad zippered HMM constructs binding to pyrene-labeled actin filaments. Zippered HMM in the presence of MgADP was mixed with a 10-fold excess of actin, and the rate of pyrene−actin fluorescence quenching was observed. (A) Hyperbolic fits of the rates (k_{obs}) of the 0-heptad zipper HMM binding to pyrene−actin in the phosphorylated (■) and dephosphorylated (○) states. (B) Normalized fluorescence transients of the phosphorylated (top curve) and dephosphorylated (bottom curve) 0-heptad zipper HMM fit to a single exponential (9.34 ± 0.04 and 13.64 ± 0.04 s^{-1}, respectively). Final concentrations of reactants: 0.33 μM HMM, 3.75 μM pyrene−actin, and 0.5 mM MgADP for the phosphorylated form and 1.25 μM HMM, 12.5 μM pyrene−actin, and 0.5 mM MgADP for the dephosphorylated form. (C) Hyperbolic fits of the rates (k_{obs}) of the 15-heptad zipper HMM binding to pyrene−actin in the phosphorylated (■) and dephosphorylated (○) states. (D) Normalized fluorescence transients of the phosphorylated (bottom curve) and dephosphorylated (top curve) 15-heptad zipper HMM binding to actin fit to a single exponential (9.40 ± 0.05 and 1.36 ± 0.04 s^{-1}, respectively). Final concentrations of reactants: 0.75 μM HMM, 7.5 μM pyrene−actin, and 0.5 mM MgADP. All experiments were performed in 20/20 buffer at 25 °C.

Table 2: Transient Kinetic Properties Describing the Interaction of HMM Constructs with Pyrene−Actin[a]

HMM construct	$1/K_1$[b] (μM)	k_{+2}[c] (s^{-1})	K_1k_{+2}[d] (μM^{-1} s^{-1})	k_{-2}[e] ($\times 10^{-3}$ s^{-1})	K_d[f] (nM)
0 HEP ZIP phos.	4.2 ± 0.3	19.0 ± 0.4	4.5 ± 0.4	7.5 ± 0.5	1.7 ± 0.4
0 HEP ZIP dephos.	8.7 ± 1.6	22.4 ± 1.6	2.6 ± 1.6	8.0 ± 0.2	3.1 ± 1.6
15 HEP ZIP phos.	3.8 ± 1.1	13.9 ± 1.0	3.6 ± 1.0	6.2 ± 0.4	1.7 ± 1.0
15 HEP ZIP dephos.	21.0 ± 12	5.7 ± 1.4	0.3 ± 0.2	7.9 ± 0.4	29.0 ± 12

[a] All experiments were performed in 20/20 buffer at 25 °C. [b] Actin concentration at which the rate of binding of myosin to pyrene−actin is half the maximal rate. [c] Maximum rate of binding of myosin to pyrene−actin. [d] Second-order rate constant for binding of myosin to pyrene−actin. [e] Rate of dissociation of myosin from pyrene−actin. [f] Rate of dissociation of myosin from pyrene−actin.

The hyperbolic dependence of the rates of actin binding on actin concentration was quite similar for the 0-heptad zipper HMM in the phosphorylated and dephosphorylated states. However, in the dephosphorylated state, the actin association rates (K_1k_{+2} = 2.6 ± 1.6 and 4.5 ± 0.4 μM^{-1} s^{-1}, respectively) as well as the affinities for actin (K_d = 3.1 ± 1.6 and 1.7 ± 0.4 nM, respectively) were reduced 2-fold compared to those for the phosphorylated state.

The actin binding properties of the 15-heptad zipper HMM construct were dramatically affected by the phosphorylation state. In the dephosphorylated state, the actin association rate (K_1k_{+2} = 0.3 ± 0.2 and 3.6 ± 1.0 μM^{-1} s^{-1}, respectively) and actin affinity were reduced ~10-fold (K_d = 29 ± 12 and 1.7 ± 1.0 nM, respectively), and the maximal rate of actin binding (k_{+2} = 5.7 ± 1.4 and 13.9 ± 1.0 s^{-1}, respectively) was reduced 3-fold compared to that of the phosphorylated state. This result is in agreement with a previous report that determined the rate of actin binding and actin affinity are reduced in the dephosphorylated state of the proteolytically prepared HMM (*16*).

DISCUSSION

The purpose of these studies is to test the stability of the S2 rod. We do this by creating strain that tends to separate the head−rod junctions, and hence uncoil S2. Two-headed binding of HMM to a single actin filament tends to create large strain separating the head−rod junctions. The reason is that the helical pitch and rise of the actin filament cause the two heads, which bind to adjacent actin monomers, to point in different directions (Figure 6). This causes the two head−rod junctions to separate by approximately 9 nm (*5*) unless S2 is sufficiently stable to constrain them together. If S2 uncoils in wild-type HMM, then zippering the S2 with a leucine zipper would either prevent two-headed binding or greatly reduce its binding affinity. Consequently, we examine whether zippered HMMs can bind via two heads and, if so,

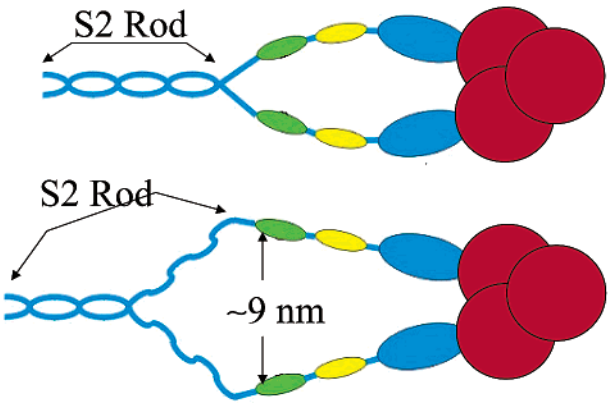

FIGURE 6: Two models of two-headed HMM binding to an actin filament. (Top) S2 remains coiled, and one or both myosin heads are distorted. (Bottom) S2 unwinds, separating the head−rod junctions by 9 nm and leaving both heads undistorted. In both models, strain (either on S2 or the heads) is caused when both heads are bound and follow the actin helical twist and rise: catalytic domain (blue oval), actin (red), essential light chain (yellow), and regulatory light chain (green). The results presented here for smooth HMM, and those presented previously for skeletal HMM (*5*), support the model where the S2 rod remains coiled (top) and, by inference, that one or both myosin heads are distorted, keeping the head−rod junctions close together.

their affinity compared to that of wild-type HMM. If two-headed binding occurs, and S2 remains coiled, then one or both of the myosin heads must distort themselves.

Two important conditions must be met. First, the HMM must remain intact, i.e., be dimerized. Figure 2 shows that all of our zippered HMM constructs are indeed dimerized. Second, the actin concentration must be kept sufficiently low to prevent two-headed binding between actin filaments. HMM binding between actin filaments would not be expected to create significant strain on S2, and hence, the actin concentration is kept $\ll$100 μM (typically $\sim$1 μM), to avoid interfilament binding (*11*). For example, at 1 μM actin, $\sim$99% of heads are expected to be bound to the same actin filament, and only $\sim$1% bound between two different filaments.

Figure 3 and Table 1, which use steady-state fluorescence quenching of pyrene−actin by myosin, show that a titration of all zippered HMMs, as well as wild-type skHMM, leads to a saturation binding stoichiometry of one HMM per two actin monomers. Wild-type skeletal HMM binding and S1 binding in rigor serve as controls for two- and one-headed binding, respectively. They also act as further checks on the actin concentration, in addition to the absorption measurements of actin stock solutions. It is well-known that wild-type HMM (both skeletal and smooth) can bind with both heads to adjacent actin monomers of an actin filament in rigor (*11*). These results therefore provide strong evidence that these zippered HMMs can bind to actin via both heads in rigor.

Via steady-state fluorescence, we also tested binding of HMM to actin in the presence of saturating levels of ADP. The motivation for studying the effect of ADP is severalfold. (1) While Figure 3 shows that zippered HMMs can bind by two heads to actin in rigor, the binding constant of wild-type HMM in rigor is sufficiently high that the zippered HMMs may still bind by two heads but with a significantly lower binding constant, due to, for example, an unzippering of S2. Adding saturating levels of ADP lowers the binding constant for binding of smooth muscle S1 myosin for actin by roughly 5-fold (*15*). (2) With ADP, the light chain domain position of smooth myosin is rotated compared to that in rigor (*19*), and hence, it is possible that the strain on S2 upon two-headed binding to actin might be different in rigor and with ADP. (3) The position of the light chain domain of smooth ADP-myosin is similar to that of rigor skeletal myosin, which we previously tested (*5*), and we found that the S2 did not uncoil. (4) There has been controversy whether both heads of HMM can bind to actin in the presence of ADP. Several reports concluded that wild-type smooth HMM can bind via two heads to actin in the presence of ADP (*20*−*22*), although one report concluded only one-headed binding can occur (*18*).

Figure 4 and Table 1 strongly support the conclusion that all the zippered smHMMs can bind to actin via two heads in the presence of ADP. Since the 15-heptad zippered HMM is functionally nearly identical to wild-type smHMM (*2*), our results support previous studies that found two-headed binding of wild-type smHMM in the presence of ADP.

The most straightforward interpretation of the steady-state fluorescence data in rigor and with a saturating level of ADP is that S2 of native HMM does not uncoil, even under the strain of two-headed binding, and hence, the zippered HMMs can readily bind to actin via both heads. An alternative possibility is that S2 uncoils, even in the zippered HMMs, allowing two-headed binding. However, in this case, the binding of the zippered HMM to actin should be dramatically lower for those zippered constructs where the zipper would have to come apart to allow two-headed binding. For example, if S2 uncoiling out to the first heptad were required, then the 0- and 1-heptad zippered HMMs should bind more weakly than the HMMs zippered at the second and fifteenth heptad. To test this hypothesis, we compared the actin binding constant (and kinetics of binding) of the 0- and 15-heptad HMM using stopped-flow measurements.

In the phosphorylated, or "on" state of myosin, we found the rates and equilibrium constant of smooth muscle myosin binding to actin were very similar for the 0- and 15-heptad zippered HMMs. The similarity in rates is consistent with a previous report which found that the maximum rates of actin binding were very similar for a proteolytically prepared smooth muscle myosin HMM, compared to those of 2- and 7-heptad zippered HMMs (*16*). Most notable is our observation that the constant for binding to actin is virtually identical for the 0- and 15-heptad zippered HMMs (K_d = 1.7 nM), and similar to that reported for wild-type HMM (*18*). The free energies of binding are therefore virtually identical, yet the free energies of uncoiling of the 0- and 15-heptad zippered HMMs are dramatically different. Therefore, our results, as well as a previous report (*16*), demonstrate that stabilizing the coiled coil at various positions does not affect the actin binding kinetics. This strongly suggests that unwinding of the coiled coil does not play a role in the two-headed binding of myosin to actin. Furthermore, that the 0-heptad HMM binds as tightly as the 15-heptad HMM implies that S2 remains coiled essentially all the way to the head−rod junction. This is a somewhat surprising result because a simple model of the head−rod junction might imply that steric clashes between the two regulatory light chains on each head could lead to some unwinding.

In the unphosphorylated, or "off" state, of myosin, we found the dependence of the actin concentration on the rate of actin binding was quite different in the dephosphorylated state for the 0- and 15-heptad zipper HMM constructs. This is likely due to the phosphorylation-dependent regulation of the 15-heptad zipper construct, as discussed below, and not the effect of the differential coiling and/or uncoiling of the S2 rod in these constructs.

We can also compare the effect of phosphorylation on actin binding kinetics seen here with previous studies, which have yielded conflicting results. A recent report suggested that only a single head of HMM can bind to actin in the dephosphorylated state, but two heads can bind actin in the phosphorylated state (*18*). However, another study (*16*) demonstrated that both heads had a much weaker actin affinity in the dephosphorylated state, and one head could bind actin 2-fold slower while the other head could bind 20-fold slower in the dephosphorylated than in the phosphorylated state. Our results with the 15-heptad zipper HMM construct are similar to those of Rosenfeld et al. (*16*), who used proteolytically prepared smooth HMM, in that we observed a 2−3-fold reduction in the maximum rate of binding to actin and a more than 10-fold reduction in the affinity for actin in the dephosphorylated state compared to that for the phosphorylated state (Table 2). However, we did not observe two different rates of actin binding (i.e., a two-exponential fit of the actin binding data; see Figure 5B). The absence of a second exponential in the 15-heptad zipper HMM suggests that a longer coiled coil, present in the proteolytically prepared HMM, may be necessary to cause two different rates. These two actin binding rates presumably arise from an interaction between the head(s) and the S2 rod that results in an asymmetry between the two heads, causing one rate to be different from the other. Such an interaction has been proposed to be involved in the phosphorylation-dependent regulation of smooth muscle myosin (*2*). Interestingly, the phosphorylation-dependent reduction in the rate of actin binding was only present in the 15-heptad zipper HMM construct, as the maximum rate of actin binding and actin affinity of the 0-heptad zipper HMM construct were not significantly affected by the phosphorylation state. Therefore, a minimal length of the rod, to provide direct head−rod interactions and/or a certain degree of flexibility in the coiled coil, may be required to cause the reduced rate of actin binding in the dephosphorylated state. The structure of smooth muscle myosin HMM suggests that there is an interaction between the two heads in the dephosphorylated state (*23*), but it is unknown whether flexibility in the coiled coil is required for this interaction.

Our results suggest that uncoiling of S2 does not play a physiological role. To enable two-headed binding of myosin to actin, there may instead be a large amount of flexibility in the myosin head itself. Rod−head interaction, and/or flexibility in the S2 rod (*24*), may also play a role in head−head interactions to facilitate proper regulation and optimal mechanical performance (*2*). For example, one study that measured unitary displacements of the 0- and 15-heptad zipper constructs found that the 15-heptad construct was similar to the wild-type HMM construct, while the 0-heptad construct had both positive and negative displacements with the average displacement being near zero (*1*). A two-dimensional crystal of unphosphorylated HMM interacting with actin was interpreted to require a bend in S2 (*23*). Thus, although the unwinding of the coiled coil is not necessary for two-headed binding of mysin to actin, flexibility and/or rod−head interaction may be necessary for obtaining optimal mechanical performance in smooth muscle myosin.

ACKNOWLEDGMENT

We thank Roger Cooke and Kathy Franks-Skiba for the gift of skeletal HMM and S1 and James Stull for the gift of myosin light chain kinase.

REFERENCES

1. Lauzon, A. M., Fagnant, P. M., Warshaw, D. M., and Trybus, K. M. (2001) *Biophys. J. 80*, 1900−1904.
2. Trybus, K. M., Freyzon, Y., Faust, L. Z., and Sweeney, H. L. (1997) *Proc. Natl. Acad. Sci. U.S.A. 94*, 48−52.
3. Wu, X., Clack, B. A., Zhi, G., Stull, J. T., and Cremo, C. R. (1999) *J. Biol. Chem. 274*, 20328−20335.
4. Wahlstrom, J. L., Randall, M. A., Jr., Lawson, J. D., Lyons, D. E., Siems, W. F., Crouch, G. J., Barr, R., Facemyer, K. C., and Cremo, C. R. (2003) *J. Biol. Chem. 278*, 5123−5131.
5. Chakrabarty, T., Xiao, M., Cooke, R., and Selvin, P. R. (2002) *Proc. Natl. Acad. Sci. U.S.A. 99*, 6011−6016.
6. O'Shea, E. K., Klemm, J. D., Kim, P. S., and Alber, T. (1991) *Science 254*, 539−544.
7. Adelstein, R. S., and Klee, C. B. (1981) *J. Biol. Chem. 256*, 7501−7509.
8. Trybus, K. M., and Lowey, S. (1985) *J. Biol. Chem. 260*, 15988−15995.
9. Pardee, J. D., and Spudich, J. A. (1982) *Methods Enzymol. 85*, 164−181.
10. Criddle, A. H., Geeves, M. A., and Jeffries, T. (1985) *Biochem. J. 232*, 343−349.
11. Conibear, P. B., and Geeves, M. A. (1998) *Biophys. J. 75*, 926−937.
12. Lombardi, V., Piazzesi, G., Ferenczi, M. A., Thirlwell, H., Dobbie, I., and Irving, M. (1995) *Nature 374*, 553−555.
13. Phan, B. C., Peyser, Y. M., Reisler, E., and Muhlrad, A. (1997) *Eur. J. Biochem. 243*, 636−642.
14. Taylor, E. W. (1991) *J. Biol. Chem. 266*, 294−302.
15. Cremo, C. R., and Geeves, M. A. (1998) *Biochemistry 37*, 1969−1978.
16. Rosenfeld, S. S., Xing, J., Cheung, H. C., Brown, F., Kar, S., and Sweeney, H. L. (1998) *J. Biol. Chem. 273*, 28682−28690.
17. Greene, L. (1981) *Biochemistry 20*, 2120−2126.
18. Berger, C. E., Fagnant, P. M., Heizmann, S., Trybus, K. M., and Geeves, M. A. (2001) *J. Biol. Chem. 276*, 23240−23245.
19. Whittaker, M., Wilson-Kubalek, E. M., Smith, J. E., Faust, L., Milligan, R. A., and Sweeney, H. L. (1995) *Nature 378*, 748−751.
20. Gollub, J., Cremo, C. R., and Cooke, R. (1999) *Biochemistry 38*, 10107−10118.
21. Dantzig, J. A., Barsotti, R. J., Manz, S., Sweeney, H. L., and Goldman, Y. E. (1999) *Biophys. J. 77*, 386−397.
22. Ellison, P. A., DePew, Z. S., and Cremo, C. R. (2003) *J. Biol. Chem. 278*, 4410−4415.
23. Wendt, T., Taylor, D., Trybus, K. M., and Taylor, K. (2001) *Proc. Natl. Acad. Sci. U.S.A. 98*, 4361−4366.
24. van Noort, J., van Der Heijden, T., de Jager, M., Wyman, C., Kanaar, R., and Dekker, C. (2003) *Proc. Natl. Acad. Sci. U.S.A. 100*, 7581−7586.
25. McLachlan, A. D., and Karn, J. (1982) *Nature 299*, 226−231.

BI035144F